IGRF-13 GFZ candidates

M. Rother[1], M. Korte[1], A. Morschhauser[1]. C. Stolle[1], J. Matzka[1], F. Vervelidou[2,1]

October 1, 2019

[1] Helmholtz Centre Potsdam, GFZ German Research Centre for Geosciences, Telegrafenberg, 14473 Potsdam, Germany.

[2] Université de Paris, Institut de Physique du Globe de Paris, CNRS, F-75005 Paris, France.

1 Introduction

This document outlines technical facts and roughly the results of the creation of the GFZ candidates for the IGRF-13, in particular the estimation of the parent `Mag.num` model. The three sections describing aspects of the three candidate types (DGRF, IGRF and SV) delivered.

The functionality of the parent `Mag.num` modelling is in its core the same as for the GFZ IGRF-12 candidate submission. Most of the fundamental descriptions apply to this `Mag.num` parent modelling as well, if we follow closely the technical description of the IGRF-12 candidate (*Lesur et al.* [2014]). But the modelling flow changed, after approx. five years of Swarm operation, on one hand by the mere amount of data, by some details on selection, filtering and preparation, on the other hand by the choice of a start model for the final iterations.

We decided to limit the `Mag.num` parent model estimation to the standard Swarm 1Hz vector field `SW_OPER_MAGB_LR_1B` product data, as there are known to be well-formed and low noise, and the corresponding harmonised and selected observatory hourly means data delivered as the Swarm `AUX_OBS` product by `BGS` *Macmillan and Olsen* [2013].

As both epochs, 2015 for the DGRF and a major part of 2019 are covered by processed and calibrated Swarm vector field readings, the parent model for the DGRF 2015 and IGRF 2020 is the same and the description in DGRF 2015, 2 applies to IGRF 2020 as well, if not stated otherwise.

2 DGRF 2015

2.1 Data

The `Mag.num` parent model Swarm satellite initial input data are the `SW_OPER_MAGB_LR_1B` 1 Hz vector field readings for all three satellites in the `MJD2000` time period 5079 - 7154, which is 2013-11-27 - 2019-08-03 as civil date.

The versions are of baseline 05 with versions 05 (most), 06 (occurring in the period MJD2000 6328 - 7000) and a very few version 07 (two).

The input hourly means of the `AUX_OBS` Swarm product portfolio are of baseline 01 and version 20, copied from the `ftp.nerc-murchison.ac.uk` server in August 2019. The time coverage of the various observatories may differ significantly, last observatory entries are of July 2019.

Input data are the vector data in the sensor system. For the rotation from sensor system into the target systems of the vector field data, the corresponding attitude data are used. There may be the need of a time dependent correction of this rotation. A set of Euler angles for a bin-wise constant time-dependent correction is co-estimated, as soon as the core model field and the external field parameters seems to be already appropriately stable.

2.2 Selection

2.2.1 Satellite data

The selection criteria used for these data are similar to those used in GRIMM series of models *Lesur et al.* [2008, 2010]; *Mandea et al.* [2012] and the DCO (Dedicated Core) Swarm L2 product.

The considered equatorial vector data, i.e. between $\pm 55^o$ magnetic latitude for magnetically quiet times, are rotated into SM coordinate system. Polar data are un-rotated.

Following criteria are applied:

- Positive value of the z-component of the interplanetary magnetic field (IMF-B_z).
- The minimal time between sampled points is set to 20 seconds.
- Data are selected only at local times between $23{:}00$ and $05{:}00$.
- For the special task of Euler estimation only this limit is extended to 18 - 06 local time.
- Data are selected only with the sun below the horizon at $100\ km$ above the Earth's usual reference radius of 6371.2 km.

- As external field index, the MMA_SHA_2F Swarm Level 2 product is used. The thresholds for the values and their time derivatives vary, as during the modeling process some re-selections are done with slightly tighten limits, partly to try to reduce nose, partly to reduce the data load. The upper limits of the final selections are 40nT for the values and 40nT for the time derivatives.

- Quality flags are used to select periods with acceptable accurate satellite positioning and star cameras quality. The limits chosen are heuristic and have not been changed after the long phase of the DCO modelling.

In polar regions, pole-wards of $|55^o|$ of magnetic latitude, the ECEF North, East, Centre (NEC) system is used for the vector magnetic field data.

For this polar region data, the selection criteria of the local time window and the sun position are dropped.

2.2.2 Observatory data

Very similar criteria are applied for the selection of the observatory data, but the Dst index is (traditionally) used for the parameterisation of the external field.

No observatories are dropped entirely, but a threshold controlled outlier removal was applied after a sequence of first model iterations, as soon as the individual observatory offsets and all other external field parameters seems to be settled. No outlier-neighbourhood removal (as for the satellite data) was applied.

2.3 Weights

The weights are a modified versions of the Huber weights. The weight w_j used for a given data value d_j, a set of model parameters $\mathbf{g}$ and a sensitivity matrix $\mathbf{A}$, are given in equation 1. The prior data standard deviation σ_j, and the scalar k_j and a_j are given in the table 1. If $\mathbf{g}$ is not given, $w_j = \frac{1}{\sigma_j}$.

$$w_j = \begin{cases} \frac{1}{\sigma_j} & \text{for } |d_j - \mathbf{A}_j \cdot \mathbf{g}| \leq k_j, \\ \frac{1}{\sigma_j} \left[\frac{k_j}{|d_j - \mathbf{A}_j \cdot \mathbf{g}|} \right]^{1-\frac{a_j}{2}} & \text{for } |d_j - \mathbf{A}_j \cdot \mathbf{g}| > k_j, \end{cases} \tag{1}$$

Additional there is an iterative process of outlier removal. Far outliers are removed after first iterations together with their neighbourhood (approx a few minutes), assuming that distortions are mostly coming in bursts. With decreasing residuals by improving the external field estimation and increasing validity of the model fit the hard thresholds are tightened slightly. But only a few percent of the data are removed by this scheme. Of course, equatorial and polar data are handled separately.

There is a large difference for the polar data between the X,Y and the Z component. The threshold for X and Y is finally about ± 300nT, this threshold for Z is much smaller (of about ± 100nT).

2.4 Model

Away from its sources, the magnetic field can be described as the negative gradient of potentials associated with sources of internal and external origin:

$$\begin{aligned} \mathbf{B} &= -\nabla\{V_i(\theta,\phi,r,t) + V_e(\theta,\phi,r,t)\} \\ V_i(\theta,\phi,r,t) &= a\sum_{l=1}^{L_i}\sum_{m=-l}^{l}(\frac{a}{r})^{l+1} g_l^m(t) Y_l^m(\theta,\phi) \\ V_e(\theta,\phi,r,t) &= a\sum_{l=1}^{L_e}\sum_{m=-l}^{l}(\frac{r}{a})^{l} q_l^m(t) Y_l^m(\theta,\phi) \end{aligned} \tag{2}$$

where $Y_l^m(\theta,\phi)$ are the Schmidt semi-normalized spherical harmonics (SHs). θ, ϕ, r and a are the co-latitude, longitude, satellite altitude and model reference radius, respectively, in geocentric coordinates. We use the convention that negative orders, $m < 0$, are associated with $\sin(|m|\phi)$ terms whereas null or positive orders, $m \geq 0$, are associated with $\cos(m\phi)$ terms.

For the largest wavelengths of the field generated in the core and lithosphere (here, assumed up to SH degree $L_i = 18$), the reference radius used in equation (2) is $a = 3485\ km$. The Gauss coefficients are parameterised in time from 2013 to 2020, using order six B-splines $\psi_i^6(t)$, with half-year time interval between spline nodes. The time dependence of the Gauss coefficients is therefore given by:

$$g_l^m(t) = \sum_{j=1}^{N_t} g_{lj}^m\, \psi_j^6(t), \tag{3}$$

where $N_t = 9$. For the core and lithospheric field of SH degree greater than 18, the reference radius is set to $a = 6371.2\ km$. The maximum SH degree used for modelling the field of internal origin is 30, although a time-invariant field covering all SH degrees from 25 to 80 is subtracted from the data so that only very small contributions from the lithospheric field remain unmodelled. The remaining parts of the internal field are the induced fields that are modelled using only one coefficient, for $N_e = 4$ different 6-month time intervals, scaling the internal part of the Dst index – i.e. the Dst_i. The time dependence of the Gauss coefficient $g_1^0(t)$ is therefore modified to:

$$g_1^0(t) = \sum_{j=1}^{N_t} g_{1j}^0\, \psi_j^6(t) + \sum_{j=1}^{N_e} g_{1j}^{0Dst}\, \mathcal{H}_j(Dst_i)\,, \tag{4}$$

where the function $\mathcal{H}_j(X)$ takes the value X in the time interval $[t_j : t_{j+1}]$ and is zero otherwise. For observatory data we also co-estimate crustal offsets.

The external field parameterisation also consists of independent parts. A slowly varying part of the external field model is parameterised over each 6-month time interval by a degree $l = 1$ order $m = 0$ coefficient in the Geocentric Solar Magnetic (GSM) system of coordinates, and two coefficients of SH degree $l = 1$, with orders $m = 0$ and $m = -1$ in a Solar Magnetic (SM) system of coordinates. The rapidly varying part of the external field is controlled using the external part of the Dst index – i.e. the Dst_e, and the $IMF\ \mathbf{B}_y$ time series. Here again 6-month time intervals are used. Four scaling coefficients for the Dst_e are introduced in each interval: three for SH degree $l = 1$ and orders $m = -1, 0, 1$ and one for SH degree $l = 2$ and order $m = 0$. One scaling coefficient for the $IMF\ \mathbf{B}_y$ is introduced in each time interval for SH degree $l = 1$ and order $m = -1$ in SM system of coordinates. Overall, the parameterisation of the external field is:

$$
\begin{aligned}
\mathbf{B}_e(\theta,\phi,r,t) \quad &= \\
-\mathcal{R}_{GSM} \quad \nabla \quad [\quad & r\sum_{j=1}^{N_e}\{\, q_{1j}^{0\,GSM}\, Y_1^0(\theta,\phi)\}\ \mathcal{H}_j(1) \qquad\qquad\qquad\qquad\qquad\qquad\qquad\qquad] \\
-\mathcal{R}_{SM} \quad \nabla \quad [\quad & r\sum_{j=1}^{N_e}\{\, q_{1j}^{0\ SM}\, Y_1^0(\theta,\phi) + \ q_{1j}^{-1\ SM}\, Y_1^{-1}(\theta,\phi)\}\ \mathcal{H}_j(1) \qquad\qquad\qquad\qquad\qquad\qquad] \\
-\nabla \quad [\quad & r\sum_{j=1}^{N_e}\{\ \sum_{m=-1}^{1}\ q_{1j}^{m\ Dst}\, Y_1^m(\theta,\phi) + (\frac{r}{a})q_{2j}^{0\ Dst}\, Y_2^0(\theta,\phi)\}\mathcal{H}_j(Dst_e) \qquad\qquad\qquad\qquad\qquad\qquad] \\
-\mathcal{R}_{SM} \quad \nabla \quad [\quad & r\sum_{j=1}^{N_e}\{\, q_{1j}^{-1\ IMF}\, Y_1^{-1}(\theta,\phi)\}\ \mathcal{H}_j(IMF\,\mathbf{B}_y) \qquad\qquad\qquad\qquad\qquad\qquad\qquad\qquad]
\end{aligned}
\tag{5}
$$

where $\mathcal{R}_{GSM}$ and $\mathcal{R}_{SM}$ are matrices rotating vectors defined in GSM and SM reference frames into the geocentric Earth fixed reference frame, respectively.
We used independent external field parameterisations for the satellite and observatory data. In the latter, we impose that $q_{1j}^{0\ SM}$ is set to zero to avoid co-linearities with the observatory crustal offsets.

2.5 Process

The solution is obtained after several iterations of an Iterative Re-weighted Least-Squares scheme where the square root values of the weights are given by equation 1.

The uniformity of the fit, i.e. the behaviour of the residuals as function of time is checked each after some iterations. Changing of the dumping parameters and even a re-selection with modified parameters was subsequently done.

2.5.1 Using differences

Beside the inversion using single vector magnetic field data, a version of `Mag.num` was created, which is using Swarm difference data (along and cross track) **only**. For this data set only a slight amount of damping is required and no external field estimation is done. It turns out that this data set allows an easy estimation of the secular variation but leads to an inaccurate estimation of the magnetic field coefficients of low degree. The comparison with observatory data shows often a good fit and to other models as well (not shown).

This 'Delta'-model version of the `Mag.num` model was used as a starting model for the full `Mag.num` candidate parent version.

2.6 Euler Angles

The rotation angles between magnetic field vectors in the sensor reference frame and the satellite coordinated system are estimated as constant in fix time intervals as presented in *Rother et al.* [2013]. The size of the bins in days is usually modified during the iterative process. For the `Mag.num` parent model the bin-size is 27 days. Previous `Mag.num` variants had used shorter time spans of 11 or 17 days, but after tightening the selection criteria, the bin size was increased to grant sufficient stability for the estimation. No estimation is done for a bin, if the bin population number drops below 1000, which is usually caused by gaps.

2.7 Regularisation

Regularization is only applied to part of the core field with temporal variation. In particular for the purpose of being a parent model of snapshots for the `IGRF` with its linear interpolated bins, the resulting parent model is intentionally fairly stiff. The third derivative is heavily damped everywhere (final parameter is about 30), while for the acceleration and secular variation only the first (at `MJD2000` $4748.5 \hat{=}$ 2012-12-31 12:00) and last node (at `MJD2000` $7305.25 \hat{=}$ 2020-01-01 06:00) are in the final model affected with moderate values of 0.001 and $1 \cdot 10^5$. The start values for the very first iterations are considerably higher.

2.8 Data misfit and residuals

The resulting residuals are calculated for the selected and later filtered data as input for the the modelling process.

For biases and misfits see table 1. The values are un-weighted estimates, and therefore can be strongly affected by outliers. For the modified Huber norm used for the final iterations of the parent model the influence of outliers should be narrowed.

Table 1: Satellite and observatory bias and sigmas of the `Mag.num` parent model, the first row shows the data type... $[1, 2, 3]$ are the mid- and low-latitude X, Y and Z satellite data in SM, $[11, 12, 13]$ are high-latitude satellite (Swarm) data. *N* is designating the number of data values, σ the standard deviation in nT. The negative numbers $[-1, -2, -3]$ are additional data but exclusively used for the Euler angle estimation.

Type		*N*	Bias	σ
	Satellite			
1	X_{SM}	266258	0.023	2.936
2	Y_{SM}	266258	-0.045	3.091
3	Z_{SM}	266258	0.215	3.215
11	X_{HL}	773163	-1.892	37.740
12	Y_{HL}	773163	1.380	44.129
13	Z_{HL}	773163	-0.727	14.084
	Satellite for Euler estimation only			
-1	X_{SM}	226619	0.173	3.989
-2	Y_{SM}	226619	-0.125	3.695
-3	Z_{SM}	226619	-0.186	3.784
	Observatories			
6	X_{SM}	516072	0.184	3.634
7	Y_{SM}	516072	-0.136	3.737
8	Z_{SM}	516072	-0.038	5.107
16	X_{HL}	114321	-0.541	10.432
17	Y_{HL}	114321	0.220	9.098
18	Z_{HL}	114321	-0.408	12.923

2.9 DGRF candidate

The DGRF GFZ candidate is just the snapshot of the dedicated final Mag.num parent model for epoch 2015.0.

3 IGRF-2020 technical description

As the parent model of the IGRF 2020, all descriptions for the DGRF-2015 apply.

3.1 IGRF 2020 candidate

As the last node of the spline representation is just covering the 2020.0 epoch, the last node interval is already at least sparsely populated and the Mag.num model is intentionally quite stiff anyhow, a snapshot of the model for epoch 2020.00 is used as predicted IGRF 2020 candidate. No forecasting is applied.

4 IGRF-SV candidate for 2022.5

A trade-off between long term drifts, the significant SV amplitude on intermediate wavelengths and the contrasting short term drifts found during the still short, allocated Swarm mission period would be respected by linear and polygon fits including a recent part of the DGRF/IGRF time series. Finally none of these fits over different time windows and subsequent extrapolation gained superiority over a simple choice: the SV of the parent model at epoch 2019.0. The SV of the parent model at epoch 2019.0 is justified due to a good data coverage at this epoch. We do not consider the evolution of the geomagnetic field being predictable, but we consider the most recent estimate of SV as a good proposal for the IGRF−SV candidate for 2022.5. We therefore propose the SV of the parent model at epoch 2019.0 as IGRF−SV candidate for 2022.5.

See Figure 2.

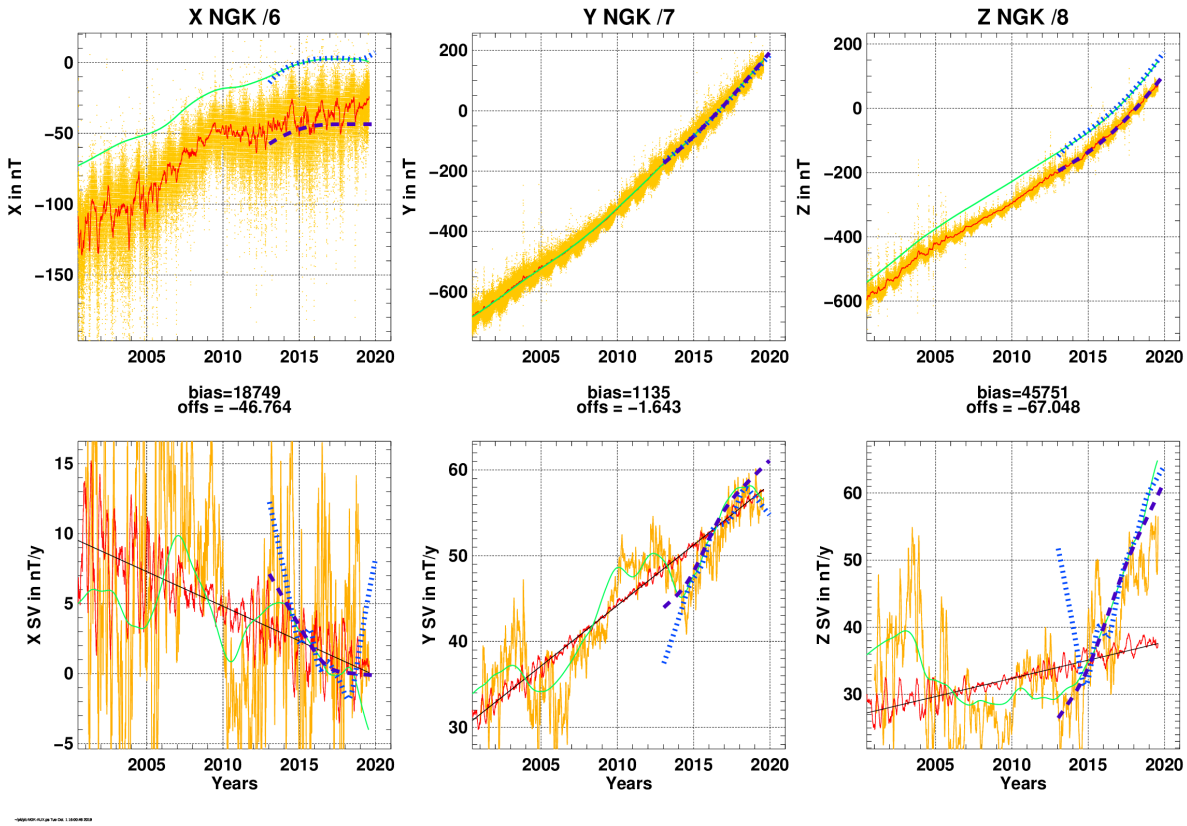

Figure 1: Example showing the relationship between noise, overlaid signal, long term drift and late model fits for the Niemegk observatory data from the hourly `AUX_OBS` Swarm product. Dashed blue line: `Mag.num` candidate parent, orange-yellow scatter: Observatory data, red and black: trend by smoothing and linear fit, green long line: `CHAOS-6-x9` model, blue dotted line: `Mag.num` by Swarm delta data (cross-track and along-track differences) only. Before plotting, the observatory bias has been applied to the `Mag.num` parent model, but neither to the CHAOS nor the `Mag.num` delta model, to better distinguish the different model estimates.

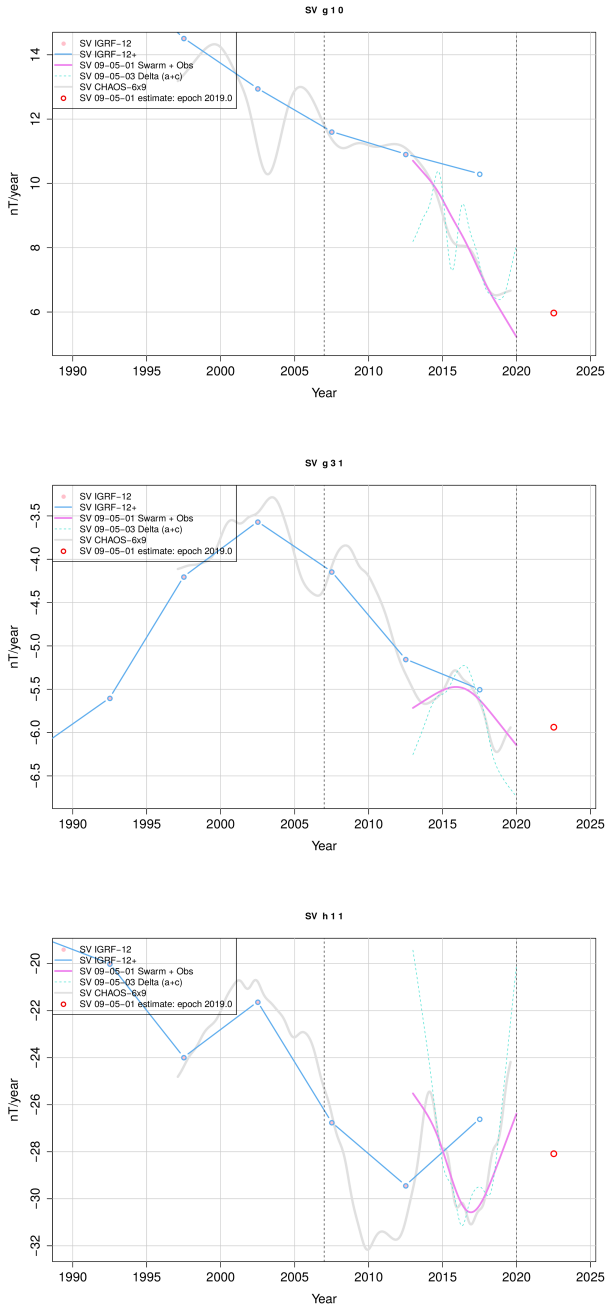

Figure 2: Three low-degree examples showing the relationship between recent `IGRF`, the `Mag.num` parent model together with a Swarm data only model. The red circle is the finally chosen predicted value, the `SV` of the parent model at epoch 2019.0.

References

Lesur, V., I. Wardinski, M. Rother, and M. Mandea, GRIMM: the GFZ Reference Internal Magnetic Model based on vector satellite and observatory data, *Geophysical Journal International*, *173*, 382–394, doi:10.1111/j.1365-246X.2008.03724.x, 2008.

Lesur, V., N. Olsen, and A. Thomson, *Geomagnetic Core Field Models in the Satellite Era*, vol. 5, chap. 11, pp. 277–294, Springer, doi:10.1007/978-90-481-9858-0, 2010.

Lesur, V., M. Rother, I. Wardinski, R. Schachtschneider, M. Hamoudi, and A. Chambodut, IGRF-12 GFZ candidates, *techreport*, Helmholtz Centre Potsdam, GFZ German Research centre for Geosciences, 2014.

Macmillan, S., and N. Olsen, Observatory data and the Swarm mission, *Earth, Planets and Space*, *65*(11), 1355–1362, doi:10.5047/eps.2013.07.011, 2013.

Mandea, M., I. Panet, V. Lesur, O. De Viron, and M. Diament, The earth's fluid core: recent changes derived from space observations of geopotential fields, *PNAS*, doi: 10.1073/pnas.1207346109, 2012.

Rother, M., V. Lesur, and R. Schachtschneider, An algorithm for deriving core magnetic field models from the swarm data set, *Earth Plan. Spa.*, *65*, 1223–1231, doi: 10.5047/eps.2013.07.005, 2013.